

# Analysis of error sources for estimating geothermal stabilised formation temperatures using analytical and rigorous methods

Espinoza-Ojeda<sup>1</sup>, OM, Santoyo<sup>2\*</sup>, E and Andaverde<sup>3</sup>, J

<sup>1</sup>Posgrado en Ingeniería (Energía), Centro de Investigación en Energía, Universidad Nacional Autónoma de México. Priv. Xochicalco s/n, Col. Centro, Temixco, Morelos 62580, México.

<sup>2</sup>Centro de Investigación en Energía, Universidad Nacional Autónoma de México, Centro de Investigación en Energía, Universidad Nacional Autónoma de México. Priv. Xochicalco s/n, Col. Centro, Temixco, Morelos 62580, México. \*Corresponding author: [esg@cie.unam.mx](mailto:esg@cie.unam.mx)

<sup>3</sup>Centro de Investigación en Ingeniería y Ciencias Aplicadas, Universidad Autónoma del Estado de Morelos. Av. Universidad No. 1001, Col. Chamilpa, Cuernavaca, Morelos 62210, México.

Analytical and rigorous solutions of 7 heat transfer models were statistically evaluated, for the estimation of stabilized formation temperatures (SFT) of geothermal wells. Linear and cylindrical heat source models were selected to represent the heat flow processes present in wells drilling operations. A statistical assessment of the main error sources involved with these models was comprehensively performed. Analytical and rigorous solutions were evaluated by using comprehensive statistical methodologies which enabled to determine the sensitivity parameters that should be considered for a reliable calculation of SFT, as well as to define the constraints where the analytical and rigorous methods provide consistent SFT estimations.

**Keywords:** Static formation temperature, bottom-hole temperatures, error propagation, shut-in time, circulation time

## Statistical methodology of evaluation

An improved statistical methodology was developed for a better evaluation of the main error sources associated with the most common heat transfer models used for estimating geothermal SFT. The methodology consisted of: (1) Selection of methods, mainly those that simultaneously propose both analytical and rigorous solutions; (2) Creation of a geothermal database with BHT and shut-in time data sets from well drilling logs and synthetic experimental works; (3) Application of different regression models (i.e., OLS and QR) with the algorithms of each selected method to calculate the SFT; (4) Statistical evaluation of the existing relationship (linear or non-linear) between BHT and the time function data of each method; (5) Comparative statistical analysis of the SFT estimates for each method based on the ratio between its analytical and rigorous solutions; and finally (6) Evaluation of accuracy in each method using a statistical comparison analyses between "true" SFT measurements and SFT estimates (inferred from analytical and rigorous solutions).

### Selection of methods

Seven methods commonly used for the determination of SFT were selected: (i) the radial source with a conductive heat flow or Brennand method (BM: Brennand 1984); (ii) the cylindrical heat source with a conductive-convective heat

flow method (CHSM) proposed by Hasan and Kabir (1994); (iii) the constant linear heat source or Horner-plot method, (HM: Dowdle and Cobb 1975; (iv) the generalized Horner or the Kutasov-Eppelbaum method (KEM: Kutasov and Eppelbaum 2005); (v) the cylindrical source with a conductive heat flow or Leblanc method (LM: Leblanc *et al* 1981); (vi) the cylindrical source with a conductive heat flow or Manetti method (MM: Manetti 1973); and (vii) the spherical and radial heat flow method (SRM) proposed by Ascencio *et al* (1994). The reader is referred to the original references of each method for more details. The analytical methods BM, HM, KEM, LM, and MM were derived from the well-known heat conduction equation (Eq. 1) under radial conditions.

$$\frac{I}{r} \frac{\partial}{\partial r} \left( r \frac{\partial T}{\partial r} \right) = \frac{I}{\alpha} \frac{\partial T}{\partial r} \quad (1)$$

whereas, the heat conduction equation under spherical-radial dimensionless coordinates (Eq. 2) was used for the SRM method,

$$\left( \frac{\partial^2 T_D}{\partial r_D^2} \right) + \left( \frac{2}{r_D} \right) \left( \frac{\partial T_D}{\partial r_D} \right) = \left( \frac{I}{\alpha} \right) \left( \frac{\partial T_D}{\partial t_D} \right), \quad 0 < r_D < \infty \quad (2)$$

The CHSM method was derived from a heat transfer model, based on transient heat exchange between drilling fluid and rock formation (Eq. 3), under conductive and convective heat flow conditions.

$$\frac{dT_w}{dt} = - \left( \frac{2\pi}{m C_{pm}} \right) \left( \frac{r_w U k}{k + r_w U T_D} \right) (T_w - T_{CHSM}) \quad (3)$$

As far as these general equations, analytical and rigorous solutions have been proposed in the literature. These solutions are summarized in Table 1 (Appendix).

### Geothermal database: BHT and shut-in time data sets

A geothermal database containing eight BHT data sets logged in geothermal borehole drilling operations and three synthetic data sets was created. The BHT data were recorded from borehole drilling reports carried out in various world geothermal sites: (1) Los Humeros geothermal field, Mexico [MXCO, Verma *et al* 2008]; (2) Mississippi petroleum wellbore, USA,

characterized by temperatures with a geothermal origin [USAM, Kutasov 1999]; (3) Larderello geothermal field, Italy [ITAL, Da-Xin 1986]; (4) Kyushu geothermal field, Japan [JAPN, Hyodo and Takasugi 1995]; (5) Norton Sound field, Alaska [COST, Cao *et al* 1988a]; (6) Chipilapa geothermal field, El Salvador [CH-A, González-Partida *et al* 1997]; (7) Roosevelt geothermal field, USA [R #9-1, Crosby 1977]; (8) Oklahoma geothermal field, USA [SGIL, Schoeppe and Gilarranz 1966].

The synthetic data sets used here were compiled from experimental works reported by Shen and Beck (1986) (SHBE), Cao *et al* (1988b) (CLAH), and Cooper and Jones (1959) (CJON). These data sets were used as they have the advantage that these experimental works reported the "true" formation temperatures (*TFT*) or SFT (i.e., SHBE = 80.0°C, CLAH = 120.0°C and CJON = 20.25°C, respectively).

For example, the thermal recovery behaviour (i.e., the BHT behaviour versus shut-in time) of some geothermal boreholes after drilling has been plotted in Figure 1 (a) (MXCO, USAM, ITAL and JAPN) and Figure 1 (b) (COST, CH-A, R #9-1 and SGIL).

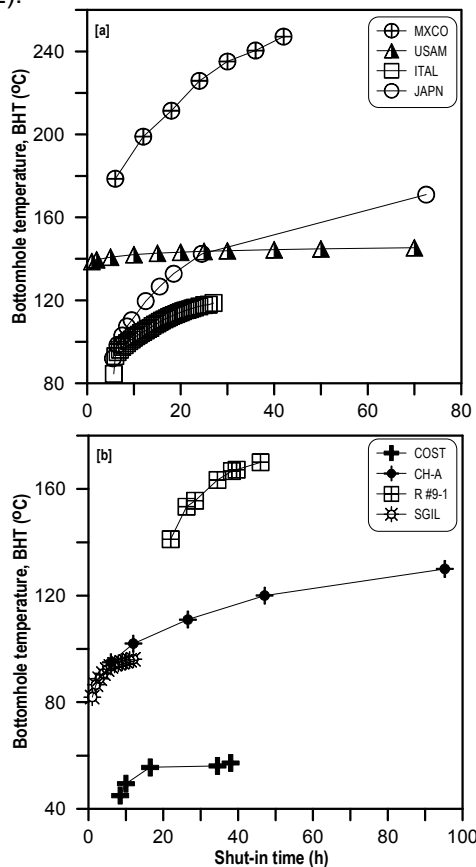


Figure 1: Temperature measurements logged after cessation of the drilling mud circulation (shut-in times).

## Regression models (OLS and QR) to calculate the SFT

OLS and QR models were initially used to evaluate either the linear or non-linear relationships between BHT and the time functions of each analytical method, and afterwards, to estimate the SFT from the eight BHT data set selected and three experimental works. For the seven analytical methods under evaluation, the independent variable  $x$  data is the time function data for each method (BMTF, CHSMTF, HMFT, KEM, LMTF, MMTF, and SRMTF),  $y$ , the dependent variable, as the *BHT*, and the intercept ( $a$  or  $a_w$ ) of any regression model (OLS and QR) will provide the SFT estimates.

### Statistical evaluation of the existing relationship between BHT and the time function data of each method

Three well-known statistical tests: (i) sequence of signs by Wald-Wolfowitz; (ii) regression using sequential subsets of an ordered array of data; and (iii) residual sum of squares (RSS); were applied to evaluate the existing relationship (linear or non-linear) between the BHT and the time function data in each analytical method used.

### Statistical comparison of the SFT estimates using the analysis of the ratio between analytical and rigorous solutions

For evaluating the prediction capability of the heat transfer models described in this work, the SFT estimates (inferred from their rigorous and analytical solutions) were statistically compared using an extension of the constant linear heat source theory suggested by Drury (1984). Such a theory was originally applied for the evaluation of the HM using the analysis of the ratio between analytical and rigorous solutions (defined as the  $\beta$  parameter), and under shut-in ( $\Delta t$ ) and circulation ( $t_c$ ) times. For these purposes,  $\beta$  parameter and the time ratio for each method was computed. A plot between  $\beta$  parameter and the time ratios ( $\Delta t / t_c$ ) was analyzed to evaluate both the similarity of the two solutions and the most suitable shut-in times for a reliable estimation of SFT. For  $\beta$  ratios close to 1, both analytical and rigorous solutions provide similar results, whereas for  $\beta$  ratio values  $> 1$  the analytical solution of the method exceeds its rigorous solution and vice versa.

### Evaluation of accuracy using statistical comparison analyses between "true" SFT measurements and SFT estimates

SFT estimates (inferred from the analytical and rigorous solutions of seven methods) were statistically compared with "true" SFT measurements reported in three synthetic experiments (SHBE, CLAH, and CJON) and a long thermal recovery history of the geothermal borehole CH-A. The accuracy of each method

was evaluated, for the first time, from statistical analyses of: (i)  $F$  and  $t$ -student statistical significance tests; (ii) deviation percentages ( $\%Dev = \{(T_p - T_m)/T_m\} \times 100$ ) between measured ("true" SFT) and SFT estimates (predicted by the solutions of the seven methods); and (iii) a linear regression analysis between "true" SFT and SFT estimates (where for an ideal linear correlation, the intercept  $a$  would be equal zero, and the slope  $b=1$ ).

## Results and discussion

Before calculating the SFT using the BHT data logged in geothermal boreholes and synthetic thermal experiments, the time functions of the seven analytical methods were calculated using their respective equations. For example, some of the resulting relationships between the BHT and the HMTF data were plotted in Figure 2, for the first group of borehole data (MXCO, USAM, ITAL, and JAPN). The plots contained in the Figure 2 show the BHT build-up curves (i.e., BHT behaviour versus time function) for the Horner analytical method. These plots were drawn with the goal to observe the existing trend between BHT and time function data. As can be observed and notwithstanding the scale effects, non-linear tendencies are clearly observed for most of the borehole and synthetic BHT-time function data, which preliminarily suggest that a non-linear regression model should be better used for a reliable determination of the SFT, instead of the linear regression model, traditionally adopted as a solution algorithm by all the analytical methods.

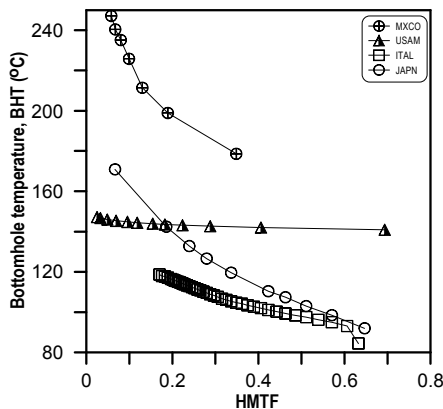


Figure 2: Plots of actual BHT measurements and time functions of the analytical Horner method.

### Use of regression models (OLS and QR) to estimate the SFT

OLS and quadratic regression algorithms were individually applied to the BHT build-up data using the equations of the analytical methods under evaluation. As with all observed phenomena, when statistical methods are assumed to apply, there are certain underlying assumptions which may not be valid. The OLS is not a statistically valid model in presence of heteroscedastic errors

(in any of the variables to be correlated  $x$  or  $y$ ), and with  $x$ - $y$  data that exhibit a non-linear trend, the OLS regression model is still used in geothermal and petroleum applications. This is basically the reason why the OLS model is still under evaluation in this work for the determination of the SFT. QR was also applied to calculate the SFT from the intercepts ( $a$ ) of the fitted QR equation ( $y = a + bx + cx^2$ ). According to the non-linear trends observed in most of the thermal recovery histories of boreholes (actual and synthetic), the QR model was a valid statistical fitting tool. The SFT estimates obtained from the OLS and QR for the seven analytical methods have been included in Table 2 (Appendix). Uncertainties of these estimates are also reported.

### Rigorous solution

Some authors have reported the rigorous solutions of five analytical methods. Such equations were analyzed and used for determining the SFT using OLS and QR regression models (see Table 3).

### Analysis of the $\beta$ ratio results

The approximate and rigorous solutions for each method were analyzed through a plot between  $\beta$  and  $(\Delta t / t_c)$  ratios to evaluate the similarity of both solutions. A BHT geothermal data set (CH-A) and the synthetic data sets (SHBE, CLAH and CJON) were used for these evaluations. Figure 3 shows some results. For  $\beta$  ratios close to 1, both approximate and rigorous solutions provide similar results. For  $\beta < 1$ , the approximate solution overestimates the SFT, whereas for  $\beta > 1$ , the approximate solution underestimates the SFT. Thus, BM, HM, and MM seem to provide acceptable results for SFT because  $\beta$  values are close to 1 for most  $(\Delta t / t_c)$  ratios (Fig. 3). On the other hand, the SRM<sub>1</sub> gives unacceptable results for most  $(\Delta t / t_c)$  ratios.

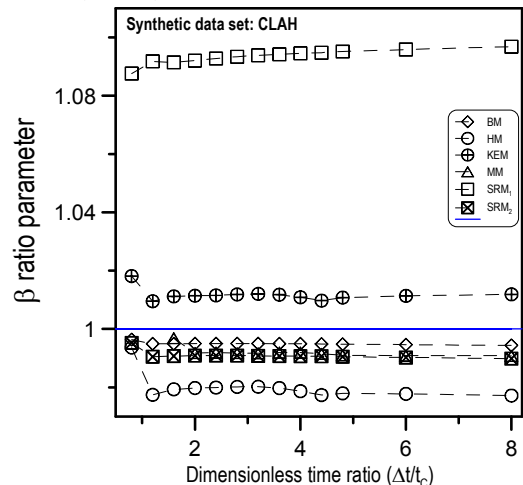


Figure 3: Plot of parameter  $\beta$  as function of ratios  $\Delta t / t_c$  for synthetic data set CLAH.

### Accuracy analysis of the SFT's calculated

A comparison of the SFT estimates provided between the OLS and QR regression models using the seven methods with three synthetic sets (SHBE, CLAH and CJON) and one geothermal set (CH-A) was carried out (see Fig. 4). For all the synthetic data sets the “true” SFT was reported (indicated as reference smoothed lines). As can be observed, for the CLAH data set using OLS, the better estimation was provided by MM, whereas for the QR model, the CHSM and MM provide the best estimations. The SRM systematically provide overestimations of the SFT in both OLS and QR models. Deviation percentages from the “true SFT” were also calculated and represented in Fig. 5.

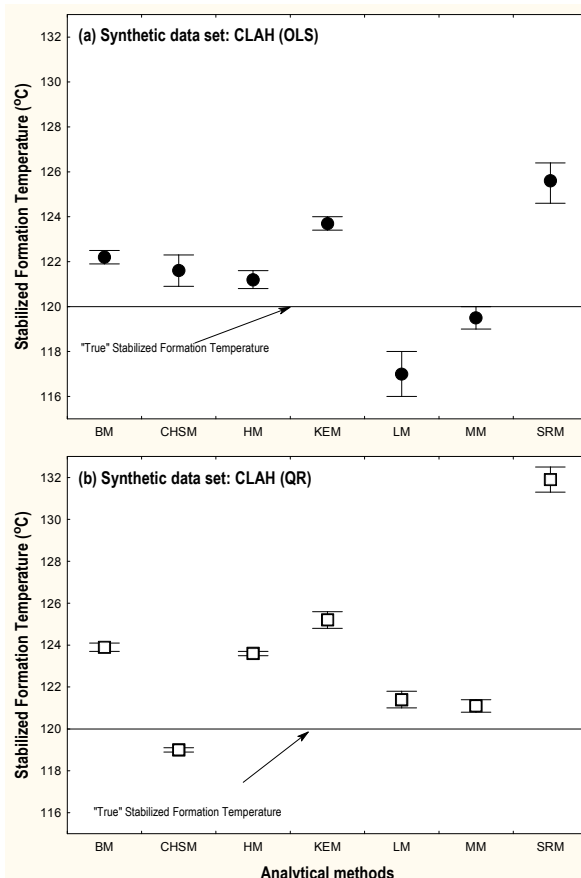


Figure 4: Accuracy evaluation of regression models (OLS and QR) for the determination of the “true” formation temperatures (SFT) using BHT synthetic data set CLAH.

### Conclusions

The empirical evaluation of error sources in heat transfer models for the determination of SFT in geothermal and petroleum wells and synthetic data sets was successfully carried out. Seven analytical methods (BM, CHSM, HM, KEM, LM, MM and SRM) were comprehensively evaluated. It was confirmed that the BHT build data logged in actual wellbore drilling operation exhibit a clear

polynomial tendency, which suggests the QR as the most suitable regression model to estimate the SFT.

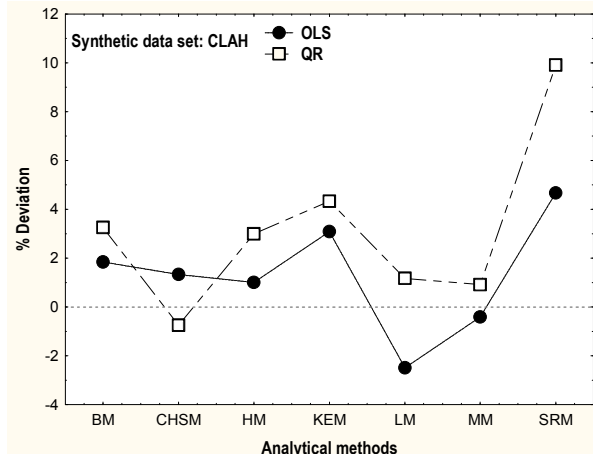


Figure 5: Results of the criterion of evaluation (% deviation) of regression models (OLS and QR) for the determination of the “true” formation temperatures (SFT) using BHT synthetic data set CLAH.

On the other hand, it was also confirmed that the OLS model, traditionally used by some analytical methods for the calculation of the SFT, is statistically an invalid regression model, and therefore must be abandoned. The  $\beta$  ratio results showed that only some approximate solutions (BM, HM, and MM) provide reliable estimations of the SFT. Shut-in and circulations times are fundamental parameters that influence the determinations of SFT, and therefore they must be measured in the field with high accuracy and precision, including the knowledge of their measurement errors.

As a final remark, further research work is still needed to develop new analytical methods with more realistic assumptions of the physical models that can reproduced the heat transfer involved in such processes.

### References

- Ascencio, F., Garcia, A., Rivera, J., and Arellano, V., 1994, Estimation of undisturbed formation temperatures under spherical-radial heat flow conditions: *Geothermics*, v. 23(4), p. 317-326.
- Brennand, A.W., 1984, A new method for the analysis of static formation temperature tests: 6th New Zealand Geothermal Workshop, New Zealand, p. 45-47.
- Cao, S., Hermanrud, C., and Lerche, I., 1988a, Estimation of formation temperature from bottom-hole temperature measurements: COST #1 well, Norton Sound, Alaska: *Geophysics*, v. 53(12), p. 1619-1621.
- Cao, S., Lerche, I., and Hermanrud, C., 1988b, Formation temperature estimation by inversion of borehole measurements: *Geophysics*, v. 53(7), p. 979-988.

Cooper, L.R., and Jones, C., 1959, The determination of virgin strata temperatures from observations in deep survey boreholes: Geophysical Journal of the Royal Astronomical Society, v. 2, p. 116-131.

Crosby, G.W., 1977, Prediction of final temperature: 3rd Workshop on Geothermal Reservoir Engineering, Stanford University, Stanford, California, p. 89-95.

Da-Xin, L., 1986, Non-linear fitting method of finding equilibrium temperature from BHT data: Geothermics, v. 15(5-6), p. 657-664.

Dowdle, W.L., and Cobb, W.M., 1975, Static formation temperature from well logs - An empirical method: Journal of Petroleum Technology, v. 27(11), p. 1326-1330.

Drury, M.J., 1984, On a possible source of error in extracting equilibrium formation temperatures from borehole BHT data: Geothermics, v. 13(3), p. 175-180.

Gonzalez Partida, E., Garcia Gutierrez, A., and Torres Rodriguez, V., 1997, Thermal and petrologic study of the CH-A well from the Chipilapa-Ahuachapan geothermal area, El Salvador: Geothermics, v. 26(5/6), p. 701-713.

Hasan, A.R., and Kabir, C.S., 1994, Static reservoir temperature determination from transient data after mud circulation: SPE Drilling & Completion, v. 9(1), p. 17-24.

Hyodo, M., and Takasugi, S., 1995, Evaluation of the curve-fitting method and the Horner-plot method for estimation of the true formation temperature using temperature recovery logging data: 20th Workshop on Geothermal Reservoir Engineering, Stanford University, Stanford, California, p. 23-29.

Kutasov, I.M., 1999, Applied Geothermics for Petroleum Engineers: Elsevier Scientific Publishing Company, First ed., 347 p.

Kutasov, I.M., and Eppelbaum, L.V., 2005, Determination of formation temperature from bottom-hole temperature logs-a generalized Horner method: Journal of Geophysics and Engineering, v. 2, p. 90-96.

Leblanc, Y., Pascoe, L.J., and Jones, F.W., 1981, The temperature stabilization of a borehole: Geophysics, v. 46(9), p. 1301-1303.

Manetti, G., 1973, Attainment of temperature equilibrium in holes during drilling: Geothermics, v. 2(3-4), p. 94-100.

Schoeppe, R.J., and Gilarranz, S., 1966, Use of well log temperatures to evaluate regional geothermal gradients: Journal of Petroleum Technology, v. 18(6), p. 667-673.

Shen, P.Y., and Beck, A.E., 1986, Stabilization of bottom hole temperature with finite circulation time and fluid flow: The Geophysical Journal of the Royal Astronomy Society, v. 86, p. 63-90.

Verma, S.P., Pandarinath, K., and Santoyo, E., 2008, SolGeo: A new computer program for solute geothermometers and application in Mexican geothermal fields: Geothermics, v. 37, p. 597-621.

## Appendix

**Table 1. Analytical and rigorous solutions of the seven analytical methods.**

Analytical method	Analytical solution	Rigorous solution
BM	$BHT(t) = T_{BM} - b_{BM} \left( \frac{1}{\Delta t + pt_e} \right)$	$T(r_w, t) = T_f - \frac{B \rho C_p r_w^2 (T_f - T_w)}{2k(\Delta t + pt_e)} \exp \left( -\frac{\rho C_p r_w^2}{4k(\Delta t + pt_e)} \right)$
CHSM	$BHT = T_{CHSM} + (b_{CHSM}) \cdot [F(t_{sD} + \Delta t_D) - F(t_D)]$	Not reported
	$T_w = T_{CHSM} - b_{CHSM} \left( e^{\frac{-\Delta t}{\lambda}} \right)$	
HM	$BHT(t) = T_{HM} + (b_{HM}) \cdot \ln((t_w + \Delta t) / \Delta t)$	$\Delta T = Q \left[ Ei \left( \frac{-r_w^2}{4\alpha \Delta t} \right) - Ei \left( \frac{-r_w^2}{4\alpha(\Delta t + t_e)} \right) \right]$
KEM	$BHT(t) = T_{KEM} + b_{KEM} \ln(X)$	$\Delta T = Q \left[ Ei \left( \frac{-r_w^2}{4\alpha \Delta t} \right) - Ei \left( \frac{-r_w^2}{4\alpha(\Delta t + t_e)} \right) \right]$
LM	$BHT(t) = T_{LM} - b_{LM} \left[ 1 - \exp \left( -\frac{r_w^2}{4\alpha \Delta t} \right) \right]$	Not reported
MM	$BHT(t) \approx T_{MM} + b_{MM} \ln \left( \frac{\Delta t}{\Delta t - t_e} \right)$	$T(t) = T_f + \frac{Q}{4\pi k} \left[ Ei \left( -\frac{r_w^2}{4\alpha \Delta t} \right) - Ei \left( -\frac{r_w^2}{4\alpha(\Delta t - t_e)} \right) \right]$
SRM	$BHT(t) = T_{SRM} + (b_{SRM}) \cdot \left( \frac{1}{\sqrt{\Delta t}} \right)$	$T_D = \frac{1}{2} \left[ erf \left[ \frac{r_D + 1}{2\sqrt{t_D}} \right] - erf \left[ \frac{r_D - 1}{2\sqrt{t_D}} \right] \right] + \frac{1}{r_D} \sqrt{\frac{t_D}{\pi}} \left[ exp \left[ -\frac{(r_D + 1)^2}{4t_D} \right] - exp \left[ -\frac{(r_D - 1)^2}{4t_D} \right] \right]$ $T_D = erf \left( \frac{1}{2\sqrt{t_D}} \right)$

**Table 2. Comparison of stabilized formation temperatures calculated by seven analytical methods (BM, CHSM, HM, KEM, MM and SRM) using eight actual BHT build-up data (MXCO, USAM, ITAL, JAPN, COST, CH-A, R #9-1 and SGIL) and three synthetic data sets (SHBE, CLAH and CJON).**

Data set	Regression model	BM	CHSM	HM	KEM	LM	MM	SRM
MXCO	OLS	254 ± 5	249 ± 2	251 ± 6	260 ± 5	249 ± 6	244 ± 6	301 ± 5
	QR	279.4 ± 3.5	253.8 ± 1.3	277.0 ± 3.5	288 ± 3	274.3 ± 3.7	269 ± 4	352 ± 16
USAM	OLS	145.7 ± 0.3	144.8 ± 0.1	146.0 ± 0.4	145.9 ± 0.3	144.8 ± 0.5	146.0 ± 0.4	147.5 ± 0.4
	QR	145.7 ± 0.3	144.7 ± 0.1	147.1 ± 0.3	147.0 ± 0.3	145.5 ± 0.4	147.1 ± 0.3	148.0 ± 0.3
ITAL	OLS	130.6 ± 0.6	127.8 ± 0.6	127.8 ± 0.6	134.2 ± 0.6	124.8 ± 0.6	120.1 ± 0.7	142.2 ± 0.6
	QR	133.4 ± 1.9	123.8 ± 1.4	132.2 ± 1.6	135.8 ± 2.5	130.0 ± 1.3	123.0 ± 0.9	161.9 ± 1.1
JAPN	OLS	172 ± 4	166.3 ± 1.8	167 ± 4	178 ± 3	162 ± 5	157 ± 7	209.9 ± 0.9
	QR	187 ± 2	169.4 ± 1.7	184.7 ± 2.5	192 ± 1	180.1 ± 3.4	162 ± 6	215
COST	OLS	60.3 ± 1.9	57.8 ± 1.4	60.0 ± 1.7	60.9 ± 2.2	59.5 ± 1.4	58.7 ± 1.0	
	QR	53.2 ± 1.2	55.8 ± 0.6	54 ± 1	51.9 ± 1.7	54.8 ± 0.7	56.3 ± 0.7	
CH-A	OLS	126.1 ± 4.3	124.8 ± 2.9	125.4 ± 4.4	128.0 ± 4.0	125 ± 5	125 ± 5	137 ± 5
	QR	134.8 ± 3.6	127.7 ± 2.7	133.0 ± 3.7	137.5 ± 3.2	133.1 ± 3.8	131.3 ± 4.1	155.5 ± 3.8
R #9-1	OLS	212.3 ± 4.1	175.1 ± 0.9	205.9 ± 3.1	216.6 ± 4.5	198.3 ± 2.1	185.5 ± 0.6	205.1 ± 0.8
	QR	156 ± 10	172 ± 1	168 ± 8	149 ± 12	178 ± 5	185.9 ± 2.4	258.4
SGIL	OLS	100.5 ± 0.1	106 ± 1	99.3 ± 0.2	102.1 ± 0.2	97.0 ± 0.4	97.5 ± 0.2	102.9 ± 0.3
	QR	100.0 ± 0.3	87.7 ± 1.4	99 ± 1	101.1 ± 0.5	99.1 ± 0.2	98.3 ± 0.2	104 ± 1
SHBE	OLS	77.7 ± 0.6	77.4 ± 0.5	75.5 ± 0.7	79.0 ± 0.5	74.1 ± 1.3	75.6 ± 0.9	83.0 ± 0.6
	QR	80.2 ± 0.2	76.2 ± 0.2	80.1 ± 0.2	81.5 ± 0.1	78.0 ± 0.6	78.5 ± 0.5	87.3 ± 0.4
CLAH	OLS	122.2 ± 0.3	121.6 ± 0.7	121.2 ± 0.4	123.7 ± 0.3	117 ± 1	119.5 ± 0.5	125.6 ± 0.8
	QR	123.9 ± 0.2	119.0 ± 0.1	123.6 ± 0.1	125.2 ± 0.4	121.4 ± 0.4	121.1 ± 0.3	131.9 ± 0.6
CJON	OLS	21.42 ± 0.27		20.76 ± 0.10	21.80 ± 0.31	20.05 ± 0.05	19.65 ± 0.11	22.41 ± 0.19
	QR	19.82 ± 0.15		20.24 ± 0.06	19.81 ± 0.14	20.22 ± 0.05	20.16 ± 0.04	20.39 ± 0.14

**Table 3. Comparison of SFT calculated by the analytical methods rigorous solutions (BM, HM, KEM, MM and SRM) using seven actual geothermal data set (MXCO, ITAL, JAPN, COST, CH-A, R #9-1 and SGIL), one petroleum data set (USAM) and three synthetic data set (SHBE, CLAH and CJON).**

Data set	Regression model	BM	HM-KEM	MM	SRM <sub>1</sub>	SRM <sub>2</sub>
MXCO	OLS	256 ± 5	254 ± 6	240 ± 6	244 ± 6	285 ± 7
	QR	281.4 ± 3.4	271 ± 11	263 ± 7	266.9 ± 3.9	342 ± 7
USAM	OLS	145.8 ± 0.3	144.4 ± 0.2	144.8 ± 0.2	144.5 ± 0.5	146.4 ± 0.4
	QR	146.8 ± 0.3	145.1 ± 0.3	145.5 ± 0.4	145.1 ± 0.4	148.4 ± 0.3
ITAL	OLS	131.7 ± 0.6	128 ± 1	120.2 ± 0.7	121.8 ± 0.6	143.8 ± 0.8
	QR	133.8 ± 2.1	127.5 ± 2.5	126 ± 1	127 ± 1	148.4 ± 4.3
JAPN	OLS	174.1 ± 3.6	159 ± 3	141 ± 4	156 ± 6	195.6 ± 3.7
	QR	188.4 ± 1.9	164 ± 8	157 ± 3	173.5 ± 4.4	219.8 ± 1.7
COST	OLS	60 ± 2	62.3 ± 2.3	60 ± 1	68 ± 6	64 ± 3
	QR	52.9 ± 1.3	56 ± 5	56.6 ± 1.2	20 ± 22	43.8 ± 3.8
CH-A	OLS	126.2 ± 4.2	118.4 ± 4.4	117.6 ± 3.9	123 ± 5	137.3 ± 4.5
	QR	135.4 ± 3.5	128 ± 5	124 ± 5	130.8 ± 4.2	156.1 ± 3.7
R #9-1	OLS	213.1 ± 4.2	202 ± 10	184.8 ± 1.2	194.9 ± 1.7	237 ± 6
	QR	154 ± 11	107 ± 23	188 ± 5	180 ± 4	118 ± 21
SGIL	OLS	101.6 ± 0.2	100.0 ± 0.2	97.9 ± 0.2	95.9 ± 0.5	103.8 ± 0.2
	QR	99.7 ± 0.4	99.6 ± 0.6	98.9 ± 0.6	97.8 ± 0.2	104.5 ± 0.7
SHBE	OLS	78.3 ± 0.5	84.7 ± 2.4	76.2 ± 0.9	72.6 ± 1.4	81.7 ± 0.9
	QR	80.4 ± 0.2	75 ± 8	78.9 ± 1.1	76.3 ± 0.8	87.4 ± 0.3
CLAH	OLS	122.8 ± 0.2	122.8 ± 0.6	118.4 ± 0.7	115.4 ± 1.1	126.9 ± 0.6
	QR	124.0 ± 0.2	121.5 ± 1.2	121.4 ± 0.4	119.5 ± 0.6	131.9 ± 0.7
CJON	OLS	21.57 ± 0.31	20.93 ± 0.23	19.77 ± 0.08	19.59 ± 0.11	20.87 ± 0.28
	QR	19.69 ± 0.18	19.85 ± 0.18	20.09 ± 0.09	19.99 ± 0.06	19.57 ± 0.29